Electronic Supplementary Material (ESI) for Dalton Transactions.

Supporting Information

Functional models of nonheme diiron enzymes: reactivity of μ-oxo-μ-1,2-peroxo-diiron(III) intermediate in electrophilic and nucleophilic reactions

Balázs Kripli, Miklós Szávuly, Flóra Viktória Csendes, and József Kaizer*

[a]*Department of Chemistry, University of Pannonia, 8201 Veszprém, Hungary*

List of Contents

1. Materials

All syntheses were done under an argon atmosphere unless stated otherwise. Solvents used for the synthesis and reactions were purified by standard methods and stored under argon. The ligand 1,3-bis(2'-pyridylimino)-isoindoline was synthesized according to published procedures.[1] Starting materials for the ligand are commercially available and they were purchased from Sigma-Aldrich. Synthesis of complex $[Fe^{II}(indH)(MeCN)_3](ClO_4)_2$ was carried out as previously reported.[2]

2. Instrumentation

The UV-visible spectra were recorded on an Agilent 8453 diode-array spectrophotometer using quartz cells.

IR spectra were recorded using a Thermo Nicolet Avatar 330 FT-IR instrument (Thermo Nicolet Corporation, Madison, WI, USA). Samples were prepared in the form of KBr pellets.

GC analyses were performed on an Agilent 6850 gas chromatograph equipped with a flame ionization detector and a 30 m SUPELCO BETA DEX 225 column.

ESI-MS samples were analyzed using triple quadruple Micromass Quattro spectrometer (Waters, Milford, MA, USA), that was operated in positive electrospray ionization mode.

NMR spectrum was recorded on a Bruker Avance 400 spectrometer (Bruker Biospin AG, Fällanden, Switzerland).

Microanalyses (elemental analysis) were done by the Microanalytical Service of the University of Pannonia.

3. Reactions of complex $[Fe^{III}_2(\mu\text{-}O)(\mu\text{-}1,2\text{-}O_2)(IndH)_2(CH_3CN)_2]^{2+}$ (1)

The μ-oxo-μ-1,2-peroxo-diiron(III) complex, $[Fe^{III}_2(\mu\text{-}O)(\mu\text{-}1,2\text{-}O_2)(IndH)_2(CH_3CN)_2]^{2+}$ (**1.(ClO$_4$)$_2$**) were prepared by adding 4 equiv of H_2O_2 to the solutions of $[Fe^{II}(IndH)\text{-}(MeCN)_3](ClO_4)_2$ (2.00×10^{-3} M) in acetonitrile (2.0 mL) at 10 °C.[2] Then, 10-50 equiv of substrates (phenylacetaldehyde (PAA), 2-phenylpropionaldehyde (PPA), cyclohexanecarboxaldehyde (CCA), propionaldehyde (PA), pivalaldehyde (TBA), *para*-substituted benzaldehydes and *para*-substituted 2,6-di-tert-butylphenols were added to the reaction solutions. All reactions were followed by monitoring UV-Vis spectral changes of the reaction solutions at 690 nm ($\varepsilon = 630\ M^{-1}\ cm^{-1}$),[3] respectively. The products (benzaldehyde, acetophenone, cyclohexanone, tert-butanol) were identified by GC, GC-MS analysis, and their yields were determined by comparison with authenic compounds using bromobenzene (or naphtalene) as an internal standard in the reactions. The acetaldehyde from the reaction mixture of **1** with PA was identified as its 2,4-dinitrophenylhydrazone by GC-MS (M+ = 224). The characterization of the product 4,4'-dihydroxy-3,3',5,5'-tetra-tert-butylbiphenyl (H2DPQ) based on previously described methods.[3]

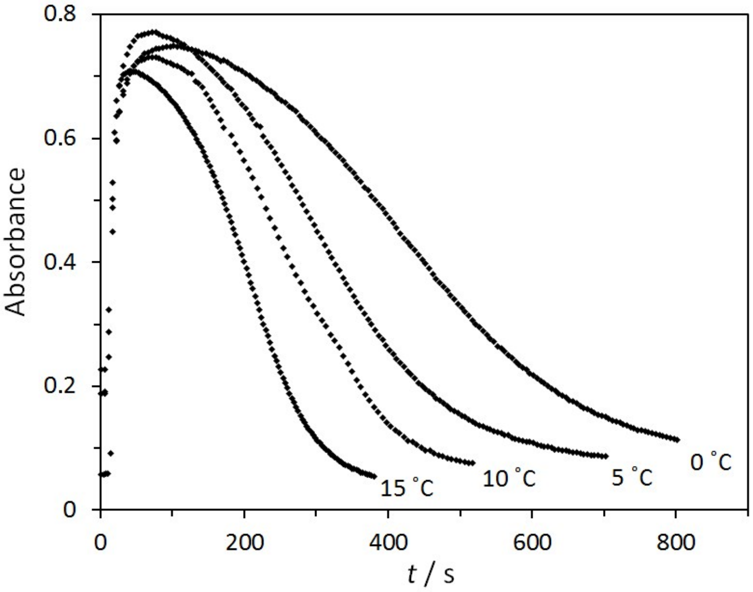

Fig. S1. Temperature-dependent stability of 1. [FeII] = 0 mM, in MeCN at 690 nm.

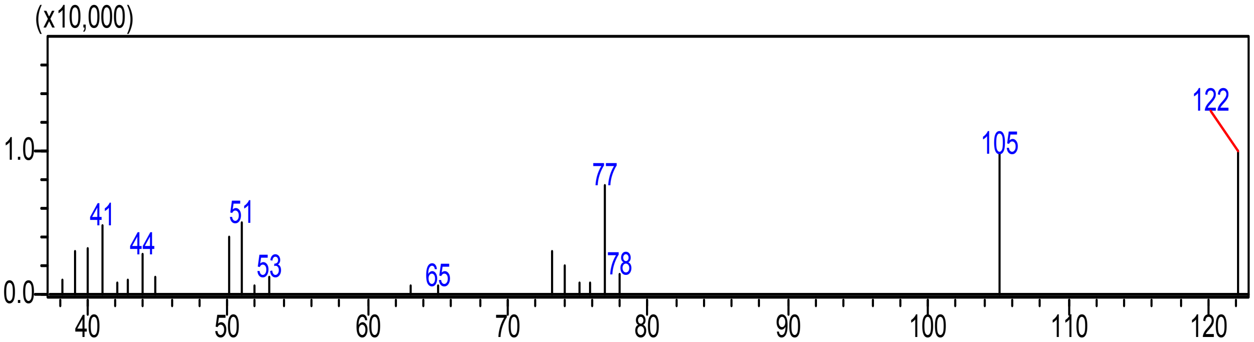

Fig. S2. Mass spectromety showing benzoic acid formation (Yields ~80-90 % based on **1**) from the reaction mixture of **1** with benzaldehyde: *m/z: 122 (100 %), 105 (97.02 %), 77 (76.67 %), 65 (5.97 %), 51 (49.48 %).*

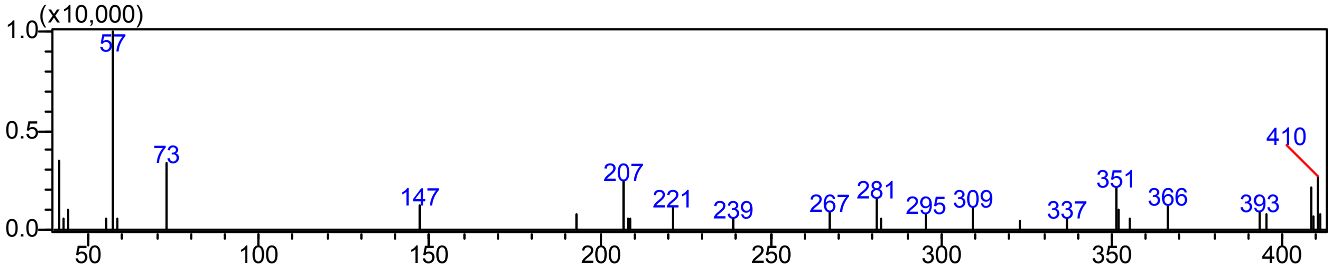

Fig. S3. Mass spectromety showing 3,3’,5,5’-tetra-*tert*-butyl-4,4’-diphenoquinone formation (Yields 80-90 % based on **1**) from the reaction mixture of **1** with 2,6-di-tert-butylphenol *m/z: 408 (26.06 %), 393 (5.79 %), 366 (9.56 %), 351 (25.08 %), 309 (11.98 %), 295 (13.03 %), 281 (17.59 %), 57 (100 %).*

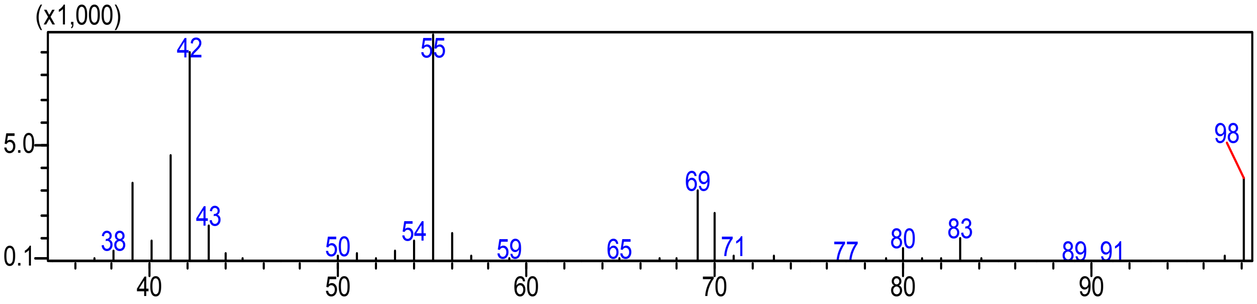

Fig. S4. Mass spectromety showing cyclohexanone formation (Yields ~60-70% based on **1**) from the reaction mixture of **1** with CCA: *m/z: 98 (35.77 %), 83 (9.86 %), 80 (5.81 %), 69 (30.55 %), 55 (100 %), 42 (90.65 %), 39 (33.87 %).*

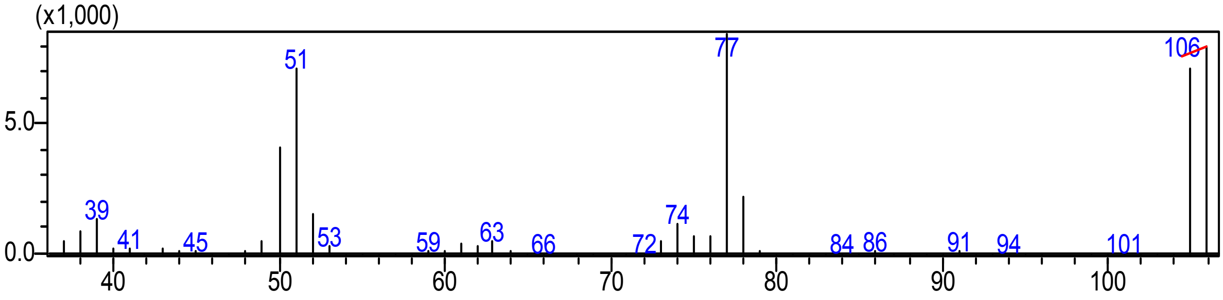

Fig. S5. Mass spectromety showing benzaldehyde formation (Yields ~50-60% based on **1**) from the reaction mixture of **1** with PAA: *m/z: 106 (79.97 %), 105 (71.12 %), 77 (100 %), 74 (11.48 %), 52 (15.07 %), 51 (71.34 %), 39 (13.55 %).*

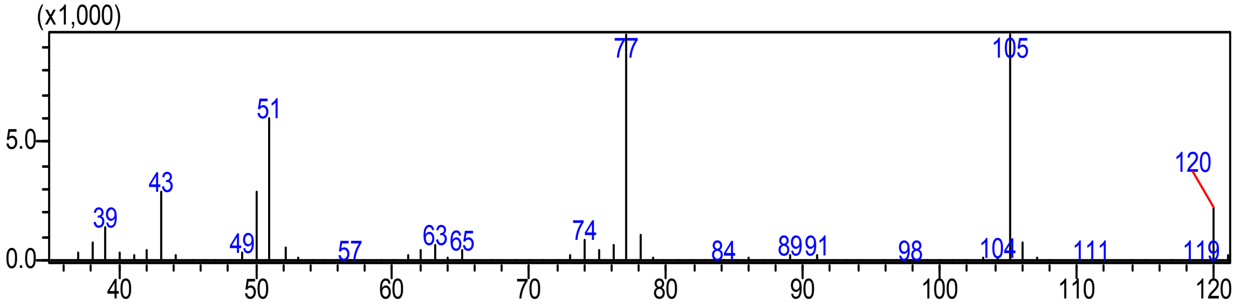

Fig. S6. Mass spectromety showing acetophenone formation (Yields ~20-30% based on **1**) from the reaction mixture of **1** with PPA *m/z: 120 (23.03 %), 106 (7.37 %), 105 (96.59 %), 79 (1.23 %), 77 (100 %), 51 (60.21 %), 43 (29.27 %), 39 (13.70 %).*

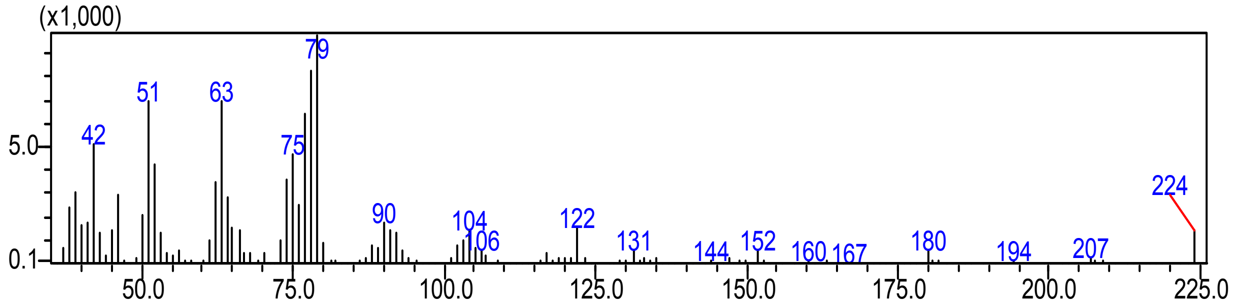

Fig. S7. Mass spectromety showing acetaldehyde-hidrazon formation (Yields ~20-30% based on **1**) from the reaction mixture of **1** with PA *m/z: 224 (14.52 %), 152 (5.16 %), 122 (14.81 %), 79 (100 %), 63 (69.53 %), 51 (69.89 %), 42 (51.12 %).*

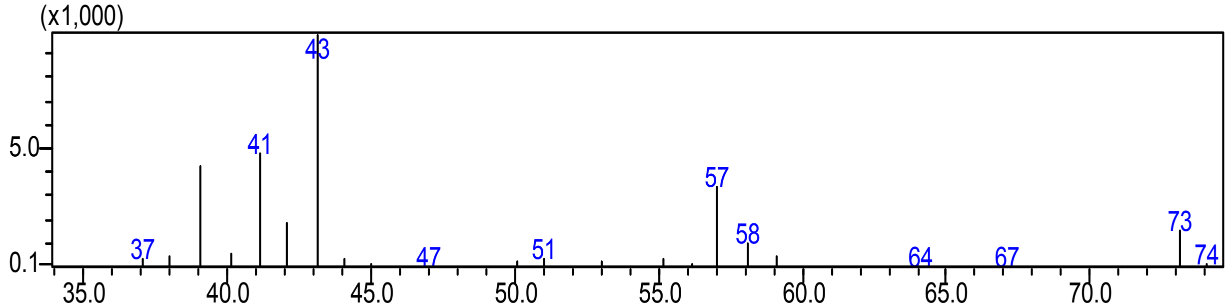

Fig. S8. Mass spectromety showing tert buthyl-alcohol (^{t}BuOH) formation (Yields ~80-90% based on **1**) from the reaction mixture of **1** with TBA *m/z: 74 (1.13 %), 73 (15.17 %), 58 (10.23 %), 57 (33.86 %), 43 (100 %), 41 (47.32 %), 39 (42.05 %), 37 (3.40 %).*

4. Kinetic data for the reaction of 1 with various aldehydes and phenols

Table S1. Kinetic data for the reaction of **1**·$(ClO_4)_2$ with benzaldehyde in MeCN at different temperatures.

N_0	T (K)	$[1]_0$ (10^{-3} M)	PhC(O)H (10^{-2} M)	k_{obs} ($10^{-2}s^{-1}$)	k_2 ($M^{-1}s^{-1}$)
1	283	1	1	3.38	2.52±0.08
2	283	1	2	5.65	2.39±0.06
3	283	1	3	7.89	2.34±0.04
4	283	1	4	10.08	2.30±0.04
5	283	1	5	12.24	2.28±0.05
6	283	1	6	15.01	2.36±0.03
7	278	1	2	4.20	1.88±0.01
8	288	1	2	5.65	2.92±0.02
9	293	1	2	11.18	3.83±0.05
10	298	1	2	15.66	4.45±0.06

Table S2. Kinetic data for the reaction of **1**·$(ClO_4)_2$ with *para*-substituted benzaldehydes in MeCN.

N_0	T (K)	$[1]_0$ (10^{-3} M)	σ_p	4R-PhCHO (0.04 M)	k_{obs} (10^{-2} s^{-1})	k_2 ($M^{-1}s^{-1}$)	log k_X/k_H
1	283	1	0.66	CN	19.74	4.72±0.08	0.305
2	283	1	0.23	Cl	11.99	2.78±0.3	0.075
3	283	1	0	H	10.08	2.30±0.4	0
4	283	1	-0.17	CH_3	8.14	1.82±0.02	-0.109
5	283	1	-0.27	OCH_3	7.55	1.67±0.02	-0.146

Table S3. Kinetic data for the reaction of **1**·$(ClO_4)_2$ with phenylacetaldehyde (PAA) in MeCN at different temperatures.

N_0	T (K)	$[1]_0$ (10^{-3} M)	PAA (10^{-2} M)	k_{obs} ($10^{-2}s^{-1}$)	k_2 ($M^{-1}s^{-1}$)
1	283	1	2	2.82	0.98±0.04
2	283	1	4	4.65	0.95±0.05
3	283	1	6	6.53	0.94±0.03
4	283	1	8	8.73	0.98±0.04
5	283	1	10	10.62	0.98±0.06
6	278	1	4	3.58	0.78±0.01
7	288	1	4	6.52	1.07±0.02
8	293	1	4	8.52	1.25±0.03

9	298	1	4	12.53	1.44±0.03

Table S4. Kinetic data for the reaction of **1**$\cdot$(ClO$_4$)$_2$ with 2-phenylpropionaldehyde (PPA) in MeCN at different temperatures.

N_0	T (K)	$[1]_0$ (10^{-3} M)	PPA (10^{-2} M)	k_{obs} (10^{-2} s^{-1})	k_2 (M^{-1}s^{-1})
1	283	1	2	2.26	0.70±0.04
2	283	1	4	3.62	0.69±0.03
3	283	1	6	5.13	0.71±0.02
4	283	1	8	6.28	0.68±0.04
5	283	1	10	7.64	0.68±0.04
6	278	1	10	5.97	0.55±0.03
7	283	1	10	10.55	0.83±0.04
8	293	1	10	13.81	1.03±0.05
9	298	1	10	18.66	1.19±0.05

Table S5. Kinetic data for the reaction of **1**$\cdot$(ClO$_4$)$_2$ with cyclohexancarboxaldehyde (CCA) in MeCN at different temperatures.

N_0	T (K)	$[1]_0$ (10^{-3} M)	CCA (10^{-2} M)	k_{obs} (10^{-2}s^{-1})	k_2 (M^{-1}s^{-1})
1	283	1	1	3.08	2.22±0.11
2	283	1	2	5.41	2.27±0.08
3	283	1	3	7.91	2.35±0.10
4	283	1	4	10.17	2.33±0.09
5	278	1	1	2.80	1.89±0.08
6	288	1	1	8.06	2.81±0.13
7	293	1	1	11.94	3.60±0.15

Table S6. Kinetic data for the reaction of **1**$\cdot$(ClO$_4$)$_2$ with propionaldehyde (PA) in MeCN at different temperatures.

N_0	T (K)	$[1]_0$ (10^{-3} M)	PA (10^{-2} M)	k_{obs} (10^{-2}s^{-1})	k_2 (M^{-1}s^{-1})
1	283	1	2	2.23	0.683±0.031
2	283	1	4	3.94	0.769±0.022
3	283	1	6	5.50	0.773±0.034
4	283	1	8	7.11	0.781±0.029
5	283	1	10	8.19	0.733±0.030
6	278	1	4	2.79	0.587±0.018
7	288	1	4	6.17	0.982±0.029

8	293	1	4	8.18	1.17±0.034

Table S7. Kinetic data for the reaction of **1**·$(ClO_4)_2$ with trimethylacetaldehyde (TBA) in MeCN at different temperatures.

N$_0$	T (K)	[1]$_0$ (10^{-3} M)	TBA (10^{-2} M)	k_{obs} ($10^{-2}s^{-1}$)	k_2 ($M^{-1}s^{-1}$)
1	283	1	1	3.70	2.84±0.11
2	283	1	2	6.86	2.99±0.12
3	283	1	3	9.18	2.77±0.09
4	283	1	4	12.92	3.01±0.13
5	278	1	3	7.77	2.44±0.09
6	288	1	3	12.18	3.32±0.15
7	293	1	3	15.93	4.14±0.18
8	298	1	3	20.88	4.71±0.17

Table S8. Kinetic data for the oxidation of DTBPH with **1.**

N$_0$	T (K)	[1]$_0$ (10^{-3} M)	DTBPH (10^{-3} M)	k_{obs} ($10^{-3}s^{-1}$)	k_2 ($M^{-1}s^{-1}$)
1	283	1	2	1.68	0.408±0.017
2	283	1	4	2.30	0.359±0.011
3	283	1	6	3.20	0.389±0.009
4	283	1	8	4.05	0.398±0.007
5	283	1	12	5.70	0.403±0.009
6	273	1	8	1.50	0.028±0.001
7	278	1	8	4.20	0.033±0.001
8	288	1	8	5.65	0.552±0.010
9[a]	273	0.5	0.04	1.65	0.031±0.001
10[b]	273	0.5	0.04	1.07	0.017±0.001

[a] $[H_2O] = 0.1$ M, [b] $[D_2O] = 0.1$ M

Table S9. Kinetic data for the oxidation of *para*-substituted phenols with **1** in MeCN at 278 K.

	k_2 10^{-2} $M^{-1}s^{-1}$	σ_p	BDE kcal mol^{-1}	σ^+
DTBPH	3.28	0	82,3	0
4Me-DTBPH	4.14	-0,17	81	-0,28
4CN-DTBPH	1.14	0,66	84,2	0,659
TTBPH	3,67	-0,20	81,2	-0,256
4-Br-DTBPH	2.24	0,23	-	0,15

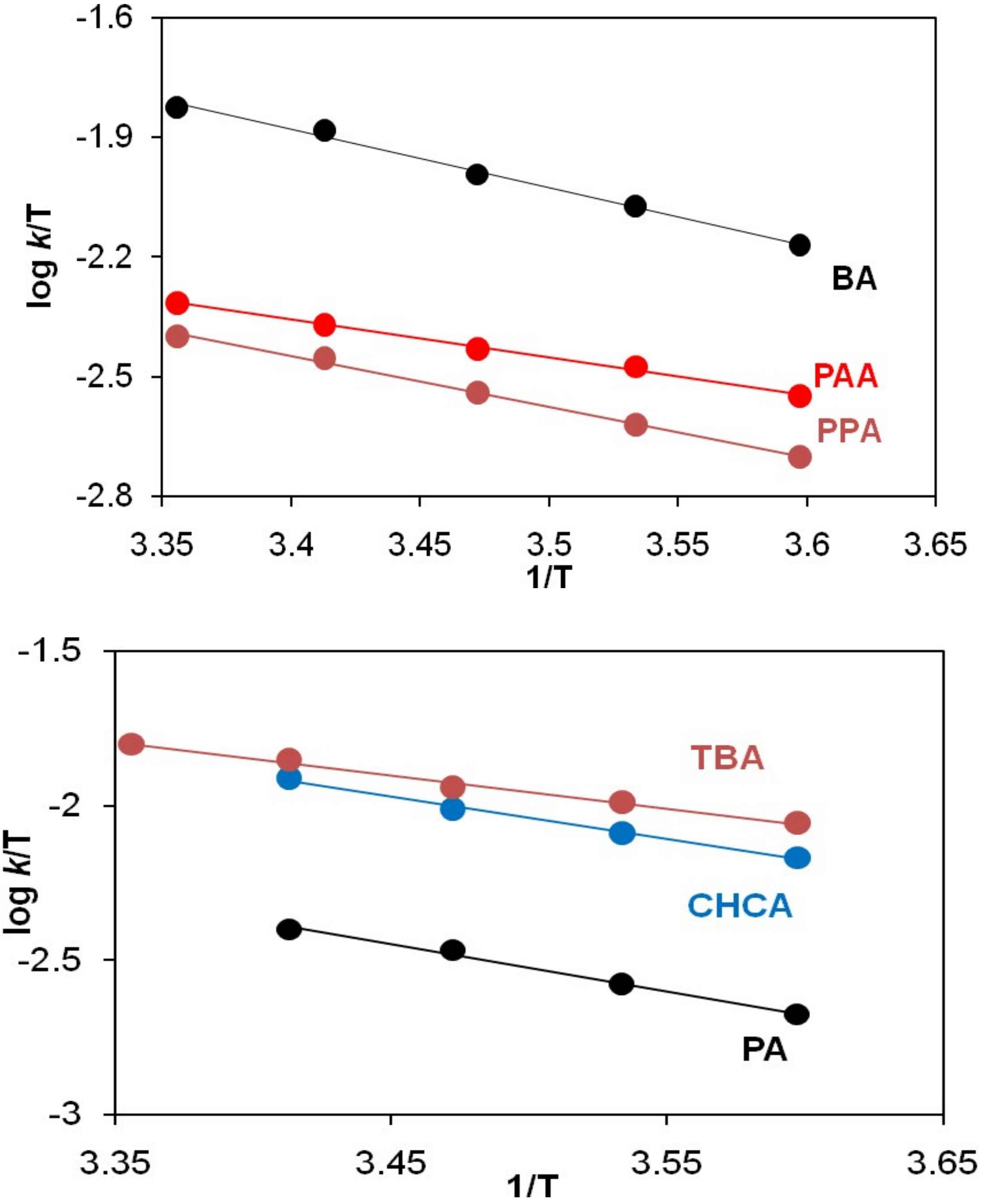

Fig. S9. Eyring plots of logk/T versus 1/T for the selected aldehydes.

1 R. Csonka, G. Speier, J. Kaizer, RSC Adv., 2015, 5, 18401.

2 J. S. Pap, M. A. Cranswick, É. Balogh-Hergovich, G. Baráth, M. Giorgi, G. T. Rohde, J. Kaizer, G. Speier, L. Que, Jr., *Eur. J. Inorg. Chem.*, 2013, 3858.

3 H. Türk, Y. Cimen, *J. Mol. Catal. A: Chem.*, 2005, **234**, 19.